Contrib. Astron. Obs. Skalnaté Pleso **56/1**, 112 – 122, (2026)
https://doi.org/10.31577/caosp.2026.56.1.112

The Baldwin effect and the Mg II - 3000 Å luminosity relation in blazars

V.M. Patiño-Álvarez[1,2], **J.U. Guerrero-González**[1], **V. Chavushyan**[1], **D.E. Monjardin-Ward**[1], **T.G. Arshakian**[3,4,5] and **I. Cruz-González**[6]

[1] *Instituto Nacional de Astrofísica, Óptica y Electrónica, Luis Enrique Erro 1, Tonantzintla, Puebla 72840, México (E-mail: victorm.patinoa@gmail.com)*

[2] *Max-Planck-Institut für Radioastronomie, Auf dem Hügel 69, D-53121 Bonn, Germany*

[3] *I. Physikalisches Institut, Universität zu Köln, Zülpicher Strasse 77, Köln, Germany*

[4] *Byurakan Astrophysical Observatory after V.A. Ambartsumian, Aragatsotn Province 378433, Armenia*

[5] *Astrophysical Research Laboratory of Physics Institute, Yerevan State University, 1 Alek Manukyan St., Yerevan, Armenia*

[6] *Universidad Nacional Autónoma de México, Instituto de Astronomía, AP 70-264, CDMX 04510, Mexico*

Received: November 1, 2025; Accepted: November 25, 2025

Abstract. We present a re-evaluation of the relationship between the Mg II λ2798 Å emission line and the 3000 Å continuum luminosity, including an analysis of the Baldwin Effect, using a sample of 40,685 radio-quiet quasars and 441 Flat Spectrum Radio Quasars (FSRQs). To address dispersion from AGN variability, we applied a binning technique after excluding over 3,000 radio-loud sources, resulting in a refined empirical correlation. Our findings reveal statistically significant differences in the slope of this relationship between RQ quasars and FSRQs, implying either intrinsic differences in their accretion disk spectra or a significant contribution from jet-induced continuum to the BLR ionization in FSRQs. Furthermore, our investigation of the Non-Thermal Dominance (NTD) parameter shows that a substantial fraction of both populations (43.8% of RQ quasars and 55.5% of blazars) exhibit $NTD < 1$. We interpret this in blazars as evidence that the accretion disk alone cannot power the BLR, while in RQ quasars, it may indicate BLR anomalies, continuum-line time lags, or UV continuum suppression by a strong corona. Finally, we demonstrate that the Baldwin Effect is a direct consequence of the fundamental line–continuum luminosity relationship.

Key words: Active galactic nuclei — Flat-spectrum radio quasars — Radio quiet quasars

1. Introduction

The luminosities of broad emission lines and their adjacent continua in Active Galactic Nuclei (AGN) are fundamentally linked, as the ionizing continuum powers the line emission from the Broad Line Region (BLR). A key phenomenon related to this is the Baldwin Effect (BE), an inverse correlation between the equivalent width of emission lines like C IV or Mg II and the continuum luminosity, first identified by Baldwin (1977). While various physical mechanisms have been proposed to explain the BE-including a softening of the ionizing continuum and the influence of metallicity or the Eddington ratio - a compelling empirical hypothesis by Patiño Álvarez et al. (2016) suggests the BE is a direct mathematical consequence of the underlying line–continuum luminosity relationship itself.

This study tests that hypothesis using large samples of 40,685 radio-quiet (RQ) quasars and 441 Flat Spectrum Radio Quasars (FSRQs), focusing on the Mg II λ2798 Å line and the 3000 Å continuum. A critical aspect of our work is the comparison between these two populations, as FSRQs possess powerful jets that can significantly contaminate the continuum, potentially altering the fundamental line–continuum connection. We employ a conservative radio-loudness threshold ($R = 10$) to ensure a clean RQ sample, minimizing jet contamination.

Our primary objectives are to: (1) re-evaluate the Mg II–3000 Å correlation, accounting for AGN variability; (2) test if the BE emerges from this correlation as predicted; (3) investigate differences between RQ quasars and FSRQs; and (4) use the Non-Thermal Dominance (NTD) parameter to identify sources where the accretion disk may not be the sole source of ionizing photons.

2. Sample selection

Our analysis utilizes two distinct samples to compare radio-quiet (RQ) quasars and Flat Spectrum Radio Quasars (FSRQs).

2.1. Radio-quiet quasar sample

We constructed a control sample of RQ quasars from the SDSS Quasar Catalog (Shen et al., 2011, hereafter *S11*). We extracted sources with measurements for the Mg II λ2798 Å line and the 3000 Å continuum, applying a strict cut for low measurement uncertainty (< 0.03 dex). After a meticulous visual inspection of spectra to identify and remove outliers with problematic data (e.g., cropped or misidentified lines), our final RQ sample contained 43,756 quasars.

An initial fit to the Mg II–3000 Å relation confirmed the parameters from *S11*. However, we found the fit to be statistically unreliable (p-value $\simeq 1$), a result we attribute to significant scatter introduced by AGN variability. Since the single-epoch SDSS observations capture objects in random activity states, the intrinsic relationship is obscured. To mitigate this, we developed a binning

technique, detailed in Section 3, which groups sources by luminosity to average out variability effects.

2.2. FSRQ blazar sample

Our FSRQ sample was drawn from the 5th Roma-BZCAT blazar catalog(Massaro et al., 2015). We cross-matched these sources with the SDSS Data Release 16 (DR16, Ahumada et al., 2020) and selected those with a redshift ($0.34 < z < 2.41$) that places the Mg II λ2798 Å line within the SDSS spectral window. This process yielded a final sample of 441 FSRQs with measurable Mg II and continuum luminosities.

2.3. Spectral analysis and measurement

To ensure a consistent comparison with the RQ sample, all FSRQ spectra were shifted to the rest frame, corrected for Galactic extinction, and trimmed to the 2500–3100 Å range.

We performed a simultaneous spectral decomposition of the continuum, Fe II emission, and the Mg II λ2798 Å line using the IRAF *specfit* task. The continuum was modeled with a power law, the Fe II emission with a template from Vestergaard & Wilkes (2001), and the Mg II line with one or two Gaussian components. This method accounts for the covariance between the continuum and line fluxes. An example of this decomposition is shown in Fig. 1.

The continuum flux at 3000 Å was measured directly from the Fe II- and line-subtracted spectrum. The total uncertainty combines the spectral noise and the SDSS calibration error. Mg II Line Flux: The line flux was obtained by integrating the spectrum over 2700–2900 Å after subtracting the continuum and Fe II emission. We rigorously estimated the uncertainty by combining three sources in quadrature: Fe II subtraction, spectral signal-to-noise, and flux calibration. Luminosities for both the line and continuum were calculated using standard cosmology. The equivalent width (EW) was computed as in Eq. 1 from the integrated line and continuum fluxes, with uncertainties propagated accordingly.

$$EW = \int_{\lambda_1}^{\lambda_2} \frac{F_\lambda - F_c}{F_c} d\lambda \tag{1}$$

To ensure that it is valid to compare our measurements to those of *S11*, we cross-matched 183 FSRQs also present in the SDSS Quasar Catalog. The parameters (continuum and line luminosities, EW) derived from our method showed excellent agreement (average differences < 0.04 dex) with the catalog values, confirming consistency. We also note that our uncertainty estimates are more comprehensive and generally larger than those in the catalog, suggesting previous uncertainties may have been underestimated.

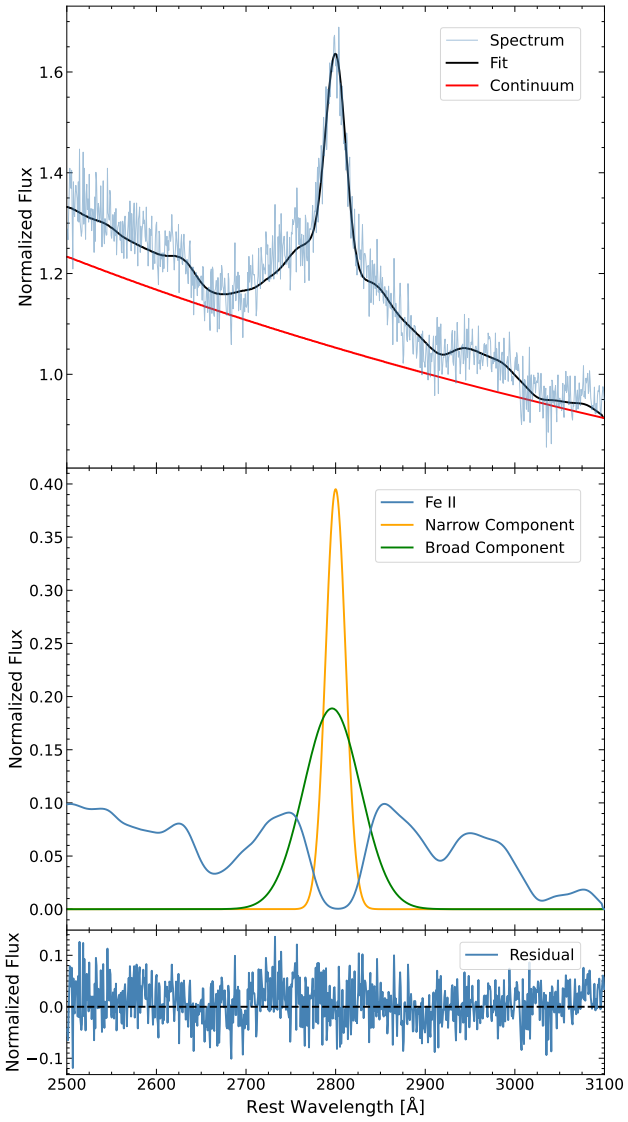

Figure 1. Example of the fitting procedure for the spectra of the FSRQ sample. The source is 5BZQ J1520+0732 (SDSS J152045.54+073230.5). Top panel: The observed spectra (blue), the final fit (black), and the power-law continuum (red). Middle panel: Spectral components fitted (excluding the continuum), including the broad Gaussian component (green), the narrow Gaussian component (orange), and the fitted Fe II emission (blue). Bottom panel: Residuals from the fit.

3. Results: line–continuum relation and the Baldwin effect

3.1. Fits to the unbinned data

We began by investigating the relationship between the Mg II line and 3000 Å continuum luminosities for our unbinned sample using three standard regression algorithms: the Bisector, Ordinary Least Squares (Y|X), and Orthogonal Distance Regression (ODR). In all three cases, the resulting linear fits yielded a p-value indistinguishable from 1.0.

A p-value of this magnitude indicates that the simple linear model does not provide a statistically significant description of the unbinned data. The model fails to reduce the residual variance meaningfully beyond the sample mean, rendering it unsuitable for its intended use in the literature: predicting one luminosity from the other for individual objects (e.g. NTD, the scaling relations of *S11*, among others). The parameters for these fits are presented in Table 1.

Table 1. Linear regression parameters for the unbinned data, following the form $\log \mathrm{L_{MgII}} = a + b \log \lambda \mathrm{L_{\lambda 3000}}$. The high p-value ($\sim 1$) for all methods indicates the models have no significant predictive power for individual sources.

Method	Slope (b)	Intercept (a)	Scatter (dex)
Bisector	0.874 ± 0.036	3.900 ± 1.671	0.2506
Y|X	0.703 ± 0.034	11.825 ± 0.767	0.2464
ODR	0.887 ± 0.019	3.266 ± 0.882	0.2530

Note. While the Y|X fit exhibits the lowest formal scatter, it assumes the independent variable ($\log \lambda \mathrm{L_{\lambda 3000}}$) is error-free and provides a non-symmetrical relation, making it less generally applicable than the Bisector or ODR methods.

The profound lack of predictive power is a direct consequence of the large intrinsic scatter in the data, which we attribute primarily to AGN variability inherent in non-simultaneous, archival observations. This finding motivates the need for an alternative approach to derive a robust relation.

3.2. Mitigating variability with binning

To address the scatter introduced by AGN variability, which rendered the linear fit on unbinned data of *S11* statistically unreliable (p-value $\simeq 1$), we applied a binning technique to both our samples. For the final sample of 40,685 Radio-Quiet (RQ) quasars, this method yielded a highly significant correlation between the Mg II and 3000 Å continuum luminosities (p-value $\simeq 0$, $r = 0.998$), as shown in the right panel of Fig. 2, and in Eq. 2. The same technique applied to the

441 FSRQs also produced a strong, statistically significant correlation (p-value $= 2.3 \times 10^{-6}$, $r = 0.986$).

$$\log L_{MgII} = (0.826 \pm 0.025) \log \lambda L_{\lambda 3000} + (6.057 \pm 0.164) \quad (2)$$

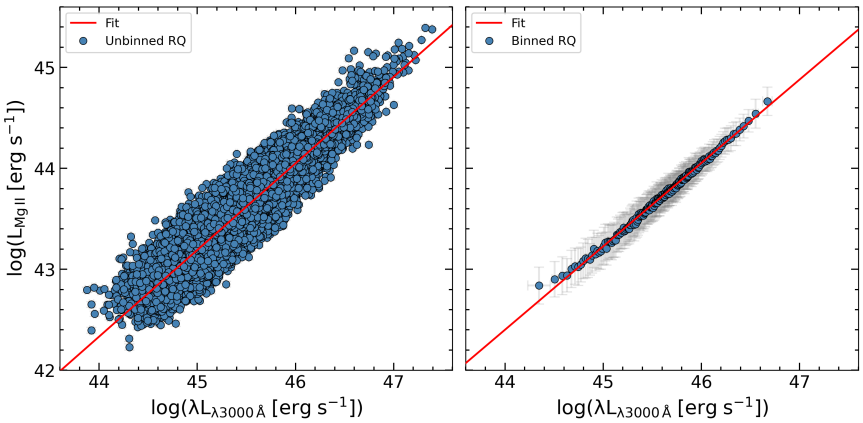

Figure 2. The relationship between the 3000 Å continuum luminosity and the Mg II λ2798 Å emission line luminosity for the RQ control sample is shown, with the unbinned data in the left panel and the binned data in the right panel. The red solid line represents the fitted relation for each data set. In the right panel, the fitted line corresponds to the relationship presented in Eq. 2.

When applying binning to the Baldwin Effect relationship for both samples, it also yields strong correlations; a Pearson correlation coefficient of -0.948, with a p-value of 10^{-101} for the RQ quasars, and a Pearson correlation coefficient of -0.913, and a corresponding p-value of 7×10^{-9} for the FSRQ sample.

3.3. A statistically significant difference in slopes

In order to statistically compare the slopes of the luminosity relations for the radio-quiet and FSRQ samples, we performed an extra sum of squares F-test. This involved comparing a model where the two samples were constrained to have a common slope against a model where they were allowed independent slopes. The test indicated that the difference in slopes was statistically significant ($F = 104.3264$, $p = 1.1102 \times 10^{-16}$).

This discrepancy cannot be explained by variability alone. We conclude that the most plausible explanation is an intrinsic difference in the source of ionization: in FSRQs, the relativistic jet likely contributes to ionizing the Broad

Line Region, thereby altering the fundamental relationship between the disk continuum and the emission lines.

4. The non-thermal dominance parameter

To quantify the jet's contribution to the continuum, we employed the Non-Thermal Dominance (NTD) parameter. The NTD compares the observed 3000 Å continuum luminosity (L_{obs}) to the luminosity predicted (L_p) by the empirical Mg II–3000 Å relation established from our RQ quasar sample. This relation defines the expected behavior for a purely disk-ionized BLR.

Based on the assumption that $L_p \simeq L_{disk}$, we can distinguish 3 clear regimes:

- $NTD > 2$: Indicates a jet-dominated continuum.
- $1 < NTD < 2$: Consistent with a disk-dominated continuum.
- $NTD < 1$: The observed continuum is fainter than predicted from the line luminosity.

Our analysis revealed a significant population of sources with $NTD < 1$ in both samples: 43.8% of RQ quasars and 55.5% of FSRQs. This result is robust, persisting even when measurement uncertainties are considered.

4.1. Interpretation of $NTD < 1$

The physical interpretation of a suppressed continuum ($NTD < 1$) differs between the two populations:

- In FSRQs (Blazars): The most plausible explanation is that the jet itself contributes to ionizing the Broad Line Region. The observed Mg II line is strengthened by this additional, non-thermal ionizing source, leading to an over-prediction of the pure-disk continuum luminosity (L_p) and resulting in $NTD < 1$. This is supported by growing observational evidence of jet-BLR interaction in individual blazars (e.g., 3C 454.3: León-Tavares et al. (2013); Isler et al. (2013); Amaya-Almazán et al. (2021); CTA 102: Chavushyan et al. (2020); B2 1633+382: Amaya-Almazán et al. (2022); Ton 599: Hallum et al. (2022)).
- In Radio-Quiet Quasars: Since significant jet ionization is unlikely, $NTD < 1$ points to intrinsic properties of the disk-BLR system. Potential explanations include: 1) Internal extinction dust in the torus or host galaxy that preferentially reddens and suppresses the UV continuum relative to the broad emission lines; 2) Anomalies in BLR structure (e.g., outflows/inflows) altering its efficiency (e.g. Popović et al., 2019); 3) Time lags between continuum variations and the BLR's response; or 4) A strong corona that diverts accretion power, suppressing the UV continuum relative to the total ionizing

flux that powers the lines (e.g. Haardt & Maraschi, 1991; Risaliti & Lusso, 2019).

5. The origin of the Baldwin effect

We tested the hypothesis that the Baldwin Effect (BE) arises naturally from the empirical relationship between the Mg II line luminosity and the 3000 Å continuum luminosity (Patiño Álvarez et al., 2016). Mathematically, the BE can be derived directly from the line-continuum relation through a change of variables, which predicts a specific link between their slopes: $B - \beta = 1$, where B is the slope of the line-continuum relation and β is the slope of the BE.

Our analysis of both the RQ and FSRQ samples confirms this prediction. The measured slopes satisfy the $B - \beta \simeq 1$ condition within uncertainties. This result demonstrates that the Baldwin Effect is an inherent feature of the line-continuum connection and does not require a separate physical explanation for its origin.

Regarding the physical origin of the non-linear line-continuum relation itself ($B \neq 1$), we identify two key factors:

1. The 3000 Å continuum as a proxy: The Mg II line responds to the ionizing continuum at $\lambda \lesssim 1621$ Å(corresponding to the 7.64624 eV ionization energy), while we observe the non-ionizing 3000 Å continuum as a practical proxy. Differences in spectral shape and variability amplitude between these bands naturally produce a non-linear relationship.

2. Time delays and BLR physics: The finite size of the Broad Line Region introduces light-travel time delays between continuum and line variations. Combined with the complex responsivity of the BLR gas, this can modify the effective slope of the relationship from the expected linear case.

These well-established AGN properties provide the physical basis for the observed non-linearity, from which the Baldwin Effect emerges mathematically.

6. Conclusions

Our analysis of the Mg II λ2798 Å line and 3000 Å continuum in 40,685 radio-quiet quasars and 441 FSRQs yields the following key conclusions:

1. A Refined Empirical Relation: By applying a binning technique to mitigate AGN variability, we have derived a robust, new empirical relation between the Mg II line and 3000 Å continuum luminosities for radio-quiet quasars, which accurately describes the underlying correlation.

2. A Fundamental Difference Between RQ Quasars and FSRQs: We find a statistically significant difference in the slopes of the line–continuum luminosity relation (and the associated Baldwin Effect) between RQ quasars and

FSRQs. This points to a fundamental physical distinction, most plausibly explained by the relativistic jet in FSRQs contributing to the ionization of the Broad Line Region.

3. The Diagnostic Power of $NTD < 1$: The Non-Thermal Dominance parameter reveals that a substantial fraction of both RQ quasars (43.8%) and FSRQs (55.5%) exhibit a continuum fainter than predicted ($NTD < 1$). In FSRQs, this signals jet ionization of the BLR. In RQ quasars, it indicates complex disk-BLR-corona physics, such as BLR anomalies, continuum-line time lags, or UV suppression by a strong corona.

4. The Origin of the Baldwin Effect: We confirm that the Baldwin Effect for the Mg II line is a direct mathematical consequence of the line–continuum luminosity relationship, requiring no separate physical mechanism to explain its existence.

Acknowledgements. J.U.G.-G. and D.E.M.-W. acknowledge support from the the CONAHCYT (Consejo Nacional de Humanidades, Ciencia y Tecnología) program for Ph.D. and M.Sc. studies, respectively. Additionally, this work was supported by the Max Plank Institute for Radioastronomy (MPIfR) - Mexico Max Planck Partner Group led by V.M.P.-A. ICG acknowledge financial support from DGAPA-UNAM grant IN-119123 and CONAHCYT grant CF-2023-G-100. This research was supported by the YSU, in the frames of the internal grant.

Funding for the Sloan Digital Sky Survey IV has been provided by the Alfred P. Sloan Foundation, the U.S. Department of Energy Office of Science, and the Participating Institutions.

SDSS-IV acknowledges support and resources from the Center for High Performance Computing at the University of Utah. The SDSS website is www.sdss4.org.

SDSS-IV is managed by the Astrophysical Research Consortium for the Participating Institutions of the SDSS Collaboration including the Brazilian Participation Group, the Carnegie Institution for Science, Carnegie Mellon University, Center for Astrophysics — Harvard & Smithsonian, the Chilean Participation Group, the French Participation Group, Instituto de Astrofísica de Canarias, The Johns Hopkins University, Kavli Institute for the Physics and Mathematics of the Universe (IPMU) / University of Tokyo, the Korean Participation Group, Lawrence Berkeley National Laboratory, Leibniz Institut für Astrophysik Potsdam (AIP), Max-Planck-Institut für Astronomie (MPIA Heidelberg), Max-Planck-Institut für Astrophysik (MPA Garching), Max-Planck-Institut für Extraterrestrische Physik (MPE), National Astronomical Observatories of China, New Mexico State University, New York University, University of Notre Dame, Observatório Nacional / MCTI, The Ohio State University, Pennsylvania State University, Shanghai Astronomical Observatory, United Kingdom Participation Group, Universidad Nacional Autónoma de México, University of Arizona, University of Colorado Boulder, University of Oxford, University of Portsmouth, University of Utah, University of Virginia, University of Washington, University of Wisconsin, Vanderbilt University, and Yale University.

References

Ahumada, R., Prieto, C. A., Almeida, A., et al., The 16th Data Release of the Sloan Digital Sky Surveys: First Release from the APOGEE-2 Southern Survey and Full Release of eBOSS Spectra. 2020, *Astrophysical Journal, Supplement*, **249**, 3, DOI:10.3847/1538-4365/ab929e

Amaya-Almazán, R. A., Chavushyan, V., & Patiño-Álvarez, V. M., Multiwavelength Analysis and the Difference in the Behavior of the Spectral Features during the 2010 and 2014 Flaring Periods of the Blazar 3C 454.3. 2021, *Astrophysical Journal*, **906**, 5, DOI:10.3847/1538-4357/abc689

Amaya-Almazán, R. A., Chavushyan, V., & Patiño-Álvarez, V. M., Multiwavelength Analysis and the C IV λ1549 Å Emission Line Behavior From 2008 to 2020 of FSRQ B2 1633+382. 2022, *Astrophysical Journal*, **929**, 14, DOI:10.3847/1538-4357/ac5741

Baldwin, J. A., Luminosity Indicators in the Spectra of Quasi-Stellar Objects. 1977, *ApJ*, **214**, 679, DOI:10.1086/155294

Chavushyan, V., Patiño-Álvarez, V. M., Amaya-Almazán, R. A., & Carrasco, L., Flare-like Variability of the Mg II λ2798 Å Emission Line and UV Fe II Band in the Blazar CTA 102. 2020, *Astrophysical Journal*, **891**, 68, DOI:10.3847/1538-4357/ab6ef6

Haardt, F. & Maraschi, L., A Two-Phase Model for the X-Ray Emission from Seyfert Galaxies. 1991, *Astrophysical Journal, Letters*, **380**, L51, DOI:10.1086/186171

Hallum, M. K., Jorstad, S. G., Larionov, V. M., et al., Emission-line Variability during a Nonthermal Outburst in the Gamma-Ray Bright Quasar 1156+295. 2022, *Astrophysical Journal*, **926**, 180, DOI:10.3847/1538-4357/ac4710

Isler, J. C., Urry, C. M., Coppi, P., et al., A Time-resolved Study of the Broad-line Region in Blazar 3C 454.3. 2013, *ApJ*, **779**, 100, DOI:10.1088/0004-637X/779/2/100

León-Tavares, J., Chavushyan, V., Patiño-Álvarez, V., et al., Flare-like Variability of the Mg II λ2800 Emission Line in the Γ-Ray Blazar 3C 454.3. 2013, *ApJL*, **763**, L36, DOI:10.1088/2041-8205/763/2/L36

Massaro, E., Maselli, A., Leto, C., et al., The 5th edition of the Roma-BZCAT. A short presentation. 2015, *Astrophysics and Space Science*, **357**, 75, DOI:10.1007/s10509-015-2254-2

Patiño Álvarez, V., Torrealba, J., Chavushyan, V., et al., Baldwin Effect and Additional BLR Component in AGN with Superluminal Jets. 2016, *Frontiers in Astronomy and Space Sciences*, **3**, 19, DOI:10.3389/fspas.2016.00019

Popović, L. Č., Kovačević-Dojčinović, J., & Marčeta-Mandić, S., The structure of the Mg II broad line emitting region in Type 1 AGNs. 2019, *Monthly Notices of the RAS*, **484**, 3180, DOI:10.1093/mnras/stz157

Risaliti, G. & Lusso, E., Cosmological Constraints from the Hubble Diagram of Quasars at High Redshifts. 2019, *Nature Astronomy*, **3**, 272, DOI:10.1038/s41550-018-0657-z

Shen, Y., Richards, G. T., Strauss, M. A., et al., A Catalog of Quasar Properties from Sloan Digital Sky Survey Data Release 7. 2011, *ApJS*, **194**, 45, DOI:10.1088/0067-0049/194/2/45

Vestergaard, M. & Wilkes, B. J., An Empirical Ultraviolet Template for Iron Emission in Quasars as Derived from I Zwicky 1. 2001, *ApJS*, **134**, 1, DOI:10.1086/320357